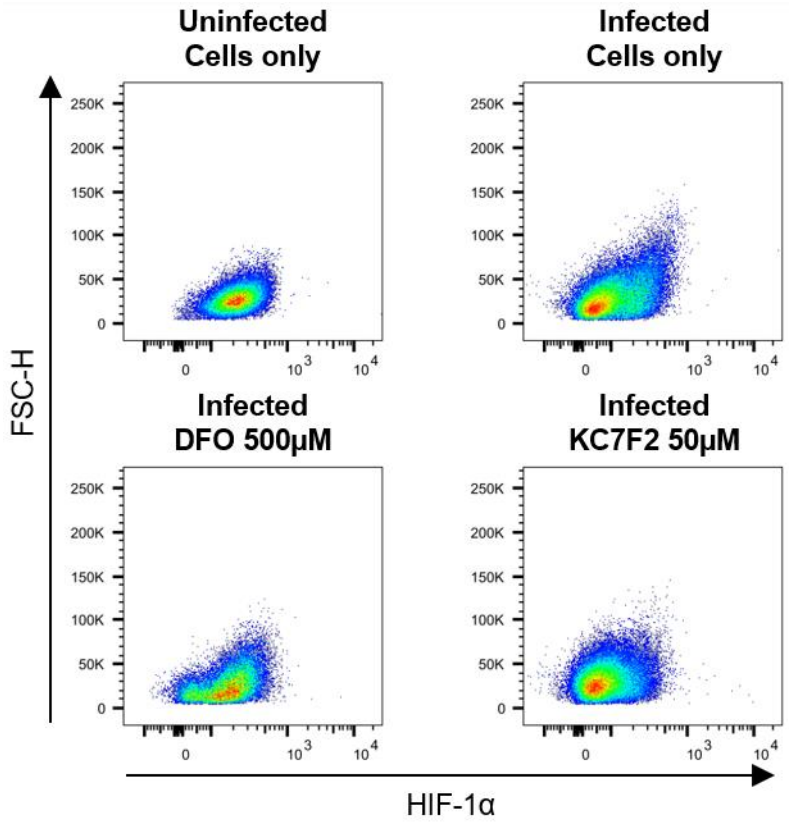

Effect of HIF-1α expression on macrophage phenotype during infection with *Mycobacterium tuberculosis*

Anouk Versnel

Report minor research internship

Master Infection and Immunity, Utrecht University

30-08-2023

Supervisors:
Dr. Susanna Brighenti, Karolinska Institutet, Stockholm
Marco Loreti, Karolinska Institutet, Stockholm

Examiner:
Prof. Dr. Linde Meyaard, Universitair Medisch Centrum Utrecht

Abstract

Tuberculosis (TB), caused by *Mycobacterium tuberculosis* (Mtb), presents a major global health challenge as antibiotic therapy is highly intensive and the occurrence of drug-resistant strains continues to increase. Therefore, there is a need for new adjunct therapies for TB. An interesting target for this is HIF-1α, a transcription factor that is involved in the cellular response towards hypoxia. Here, an *in vitro* model of human blood-derived macrophages infected with the avirulent mycobacterium strains Bacille Calmette Guérin (BCG) and H37Ra was used to study the effect of Mtb infection on the phenotype of macrophages, including polarization towards inflammatory (M1) or anti-inflammatory (M2) macrophages, as well as how this is affected by HIF-1α modulation. Additionally, the method of flow cytometry to measure HIF-1α expression was evaluated. Uninfected macrophages displayed a highly dominant M2 phenotype, which became a mixed with slightly dominant M1 phenotype after infection with BCG and H37Ra. While this seems favorable for Mtb killing, inhibitory molecules PD-L1 and IDO were upregulated, which could counteract the positive effect of M1 polarization. Stabilization or blockade of HIF-1α did not affect M1/M2 polarization of BCG-infected macrophages. However, expression of IL-1β was upregulated after stabilization of HIF-1α, which seems favorable for Mtb killing. The effect of HIF-1α stabilization and blockade could not be clearly demonstrated when visualizing HIF-1α expression with flow cytometry, but parallel western blot experiments revealed that at least HIF-1α stabilization was successful. Western blot seemed to have a higher sensitivity to detect differences in HIF-1α expression and less subject to donor variation compared to flow cytometry. All in all, additional research is needed to optimize the currently used flow cytometry protocol for the detection of HIF-1α, as well as to further characterize the effect of HIF-1α modulation on macrophage phenotype in the context of Mtb infection.

Layman's summary

Tuberculosis (TB) is caused by the bacterium *Mycobacterium tuberculosis* (Mtb) and is the leading cause of death from infectious diseases among adults, apart from COVID-19. Antibiotic treatment of TB is long and intensive, which makes it more difficult to adhere to and promotes the emergence of antibiotic-resistant Mtb strains. Therefore, there is a strong need to discover new therapies. Therapies that target the host, e.g. by influencing the immune system to better combat the bacteria, are of interest here, as resistance to these therapies is rarer in comparison to antibiotics that target the bacteria directly.

Mtb is primarily a pulmonary pathogen. The first immune cells in the lungs that are encountered by the bacteria are macrophages. The macrophages can engulf the bacteria and try to degrade them, but Mtb is often able to counteract this process and can survive and replicate in the cytoplasm of the macrophage. The ability of macrophages to combat Mtb depends on the manner in which they are differentiated. In a simplified concept, macrophages can be divided into inflammatory (M1) and anti-inflammatory (M2) phenotypes. M1 macrophages produce cytokines and other factors that are essential in TB defense, while M2 macrophages play a role in attenuating inflammation, which creates a permissive environment for TB growth. Therefore, therapies that can promote M1 polarization of macrophages are of interest for TB.

A potential target for host-directed therapy for TB is HIF-1α. This is a transcription factor that is normally involved in the response of cells to environments with low oxygen levels. Macrophages can express HIF-1α and activation of HIF-1α is known to induce expression of several factors that combat bacteria such as Mtb, including the cytokine IL-1β. Thus, stabilizing expression of HIF-1α seems to be a good avenue to improve killing of Mtb. This has also been demonstrated in several studies, but the effect of HIF-1α modulation on the phenotype of the macrophages infected with Mtb has not been studied in much detail and is the focus of this project.

A model was used where monocytes are isolated from human blood and differentiated to macrophages in the lab, after which they were infected with non-virulent strains of Mtb, namely Bacille Calmette Guérin (BCG), the vaccine strain for Mtb, and H37Ra. Uninfected macrophages had a highly dominant M2 phenotype, but after infection the phenotype became mixed and slightly in favor of M1. The M1/M2 polarization remained the same when macrophages were treated with drugs to stabilize or block HIF-1α, both in uninfected and BCG-infected macrophages.

A secondary aim was to evaluate the use of the technique flow cytometry to visualize HIF-1α expression. The expression of HIF-1α via this method was highly variable. A direct comparison with the technique western blot, which is the established method to detect HIF-1α expression, demonstrated that changes in HIF-1α expression were more clear and less subject to donor variation with western blot compared to flow cytometry.

In conclusion, the currently used protocol for HIF-1α detection with flow cytometry should be further optimized and additional research is needed to further characterize the effect of HIF-1α modulation on macrophage phenotype in the context of Mtb infection, and its potential as a target for TB therapy.

Abbreviations

BCG = Bacille Calmette Guérin

BMDMs = Bone marrow-derived macrophages

CAMP = Cathelicidin Antimicrobial Peptide

CCR7 = C-C Chemokine Receptor type 7

CD200R = CD200 Receptor

CFU = Colony-forming units

CTLA-4 = Cytotoxic T-lymphocyte-associated protein 4

DCM = Dead cell marker

DCs = Dendritic cells

DFO = Deferoxamine

DMOG = Dimethyloxalylglycine

ESAT-6 = Early Secreted Antigenic Target 6-kDa protein

FBS = Fetal bovine serum

FIH = Factor Inhibiting HIF

GFP = Green-fluorescent protein

HIF-1α = Hypoxia-Inducible Factor 1α

HRE = Hypoxia Response Elements

HRP = Horseradish peroxidase

IDO = Indoleamine 2,3-Dioxygenase

IFN-γ = Interferon-γ

iNOS = inducible Nitric Oxide Synthase

LPS = Lipopolysaccharide

M-CSF = Macrophage Colony-Stimulating Factor

MDMs = Monocyte-derived macrophages

MFI = Mean fluorescent intensity

MOI = Multiplicity of infection

Mtb = *Mycobacterium tuberculosis*

NO = Nitric Oxide

OD = Optical density

PBMCs = Peripheral blood mononuclear cells

PBS = Phosphate-buffered saline

PD-1 = Programmed Death 1

PD-L1 = Programmed Death-Ligand 1

PHD = Prolyl Hydroxylase

ROS = Reactive Oxygen Species

RT = Room temperature

RT-PCR = Real-time PCR

TB = Tuberculosis

TBS-T = Tris-buffered saline-0,05% Tween-80

TLR2 = Toll-like Receptor 2

TNF-α = Tumor Necrosis Factor α

VHL = von Hippel-Lindau

WB = Western blot

WT = Wild-type

Introduction

Mycobacterium tuberculosis (Mtb) is an intracellular bacterium and the main causative agent of tuberculosis (TB). Apart from COVID-19, TB is the leading cause of death by infectious diseases in adults. Approximately 1.6 million people died from active TB disease in 2021 and it is estimated that a quarter of the world population is carrier of a latent Mtb infection[1]. The only commercially available vaccine for TB, Bacille Calmette Guérin (BCG), is over a hundred years old. It has a highly variable efficacy and does not protect adults from pulmonary TB infection. Thus, it is difficult to prevent TB with vaccination. TB can be treated with antibiotics and is therefore considered a curable disease. However, because TB is a chronic infection that has to be treated with long and intensive antibiotic treatment, antibiotic resistance is common and at least 20% of Mtb infections occur with mono- or multidrug-resistant strains, indicating that there is a strong need for new adjunct therapies to support treatment of primarily drug-resistant TB[2,3]. Alternatives to antimicrobial treatments are so called host-directed therapies that aim to restore immune cell responses and antimicrobial effector functions as a complement to antibiotics that usually kill the bacteria directly. Such therapy could involve modulation of Mtb-infected macrophages or T cells, targeting specific pathways that impact inflammation and immunopathology, and that can limit Mtb growth and pathological inflammation at the same time as specific immune responses are enhanced[4,5].

When Mtb enters the lungs of a host, the first immune cells the bacteria encounter are alveolar macrophages. While these cells phagocytose Mtb, infection often persists as Mtb can prevent phagolysosomal fusion and bacterial degradation, allowing survival and replication inside macrophages, either in the phagosome or in the cytosol. Once adaptive immunity is activated, bacteria are usually contained in inflammatory structures called granulomas, which provide a niche for bacterial growth but at the same time prevent bacterial spread throughout the body[2]. As the primary cell type to be infected during Mtb infection, macrophages play an important role in the regulation of TB. Macrophage differentiation is complex, with multiple subtypes that can blend into each other[6]. However, a simplified concept of macrophage polarization can be described as either classically activated/inflammatory (M1) or alternatively activated/anti-inflammatory (M2), which can be distinguished by several surface markers, e.g. CD86 for M1 and CD163 for M2[7,8]. M1 macrophages produce inflammatory cytokines, reactive oxygen species (ROS), as well as nitric oxide (NO) that are essential in TB defense, while M2 macrophages play a role in attenuating inflammation and can thus permit intracellular bacterial growth[9,10]. Therefore, promoting M1 polarization of macrophages might be an interesting avenue to consider for adjunct therapies to treat TB.

A potentially interesting target for host-directed therapy is Hypoxia-Inducible Factor 1α (HIF-1α). HIF-1α is part of the HIF-family of transcription factors, which is important for the adaptation of cells to a hypoxic environment like the TB granuloma or solid tumors. Activation of HIF will induce among others a switch to glycolysis and angiogenesis, which is beneficial in physiological situations of hypoxia but in the case of a tumor can also contribute to cell survival, invasion, and metastasis[11,12]. HIF-1α is expressed in cells of the innate and adaptive immune system, including macrophages, neutrophils, dendritic cells and lymphocytes[11–13]. Generally, HIF-1α is constitutively expressed, although transcription of the *HIF1A* gene can be increased by e.g. ROS, cytokines and bacterial lipopolysaccharide (LPS)[13]. These stimuli induce *HIF1A* via the PI3K/AKT/mTOR, RAS/RAF/MEK/ERK, and IKK/NF-κB pathways, among others[12] (**Fig. 1A**). In the situation of normoxia, where a sufficient oxygen level is present for regular cell function, two proline residues on HIF-1α are hydroxylated by prolyl hydroxylases (PHD). This serves as a signal for HIF-1α to be ubiquitinated by von Hippel-Lindau (VHL) E3 ubiquitin ligase, leading to its degradation by the proteasome. In addition, Factor Inhibiting HIF (FIH) hydroxylates an asparagine residue on HIF-1α, which prevents binding of HIF-1α to its co-

activator p300/CBP and thus inhibits nuclear translocation and transcriptional activity. Both PHD and FIH depend on oxygen as its cofactor, meaning that they are not active in situations of hypoxia, which results in the stabilization and transcriptional activity of HIF-1α. HIF-1α forms a complex with HIF-1β and p300/CBP and binds to Hypoxia Response Elements (HRE) in the DNA to enhance transcription of HIF-responsive genes, including the genes encoding IL-1β, inducible Nitric Oxide Synthase (iNOS), and Tumor Necrosis Factor α (TNF-α)[11–13] (**Fig. 1B**).

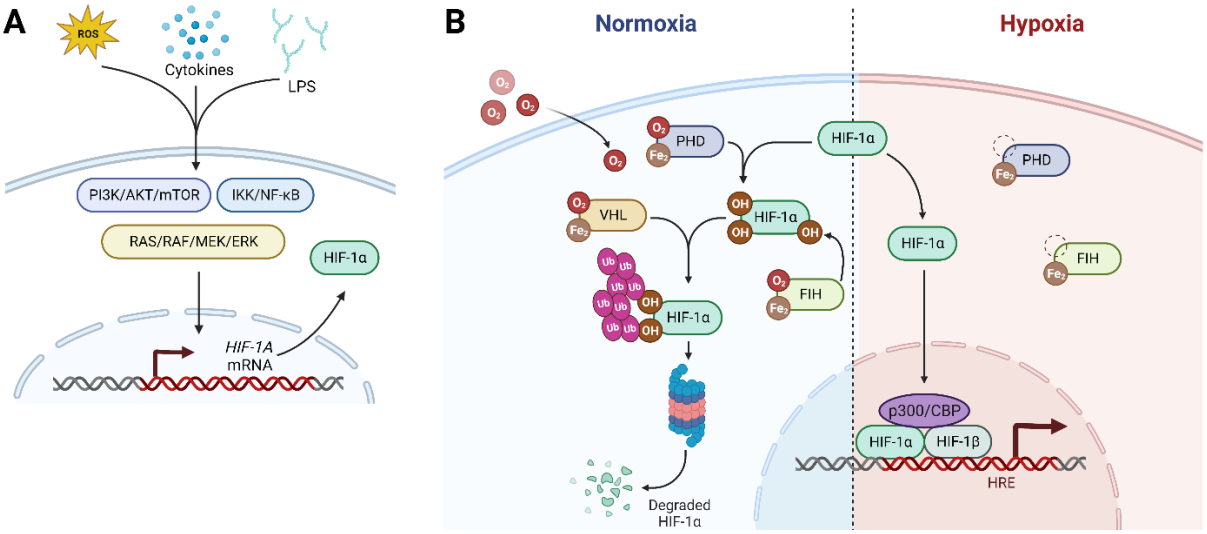

Figure 1. Regulation of HIF-1α expression. *A) Transcriptional regulation of HIF-1α. Stimuli such as ROS, cytokines and bacterial LPS can activate the PI3K/AKT/mTOR, IKK/NF-κB and/or RAS/RAF/MEK/ERK pathways. These can enhance the transcription of the* HIF1A *gene. B) Post-transcriptional regulation of HIF-1α. During normoxia, HIF-1α is hydroxylated by PHD, which serves as a signal for ubiquitination by the E3-ligase VHL. HIF-1α is then recognized by the proteasome and degraded. In addition, HIF-1α is hydroxylated by FIH which prevents the interaction of HIF-1α with its co-activator p300/CBP. During hypoxia, PHD and FIH are inactive as they lack oxygen as their cofactor. HIF-1α is free to enter the nucleus and form a complex with HIF-1β and p300/CBP. The transcription complex binds to HRE in the DNA and transcription of HIF-responsive genes is activated. Created using biorender.com.*

HIF-1α is important in the regulation of immune cell metabolism and function during bacterial infection. This was first demonstrated in mice lacking HIF-1α in the myeloid lineage[14]. Neutrophils and macrophages of these mice developed normally, but in a hypoxic environment the switch to glycolysis was strongly impaired. Functionally, this led to decreased aggregation, motility and invasion in macrophages, in addition to reduced intracellular killing of bacteria[14]. Macrophages have also been the focus of HIF-1α research in the context of Mtb infection, as alveolar macrophages are the primary cell type to be infected by Mtb[3]. Generally, bone marrow-derived macrophages (BMDMs) or human monocyte-derived macrophages (MDMs) show increased HIF-1α expression both at the protein and mRNA level after infection with BCG or the virulent strain H37Rv[15–18]. Several *in vitro* studies demonstrate that blocking HIF-1α expression in macrophages is detrimental for Mtb control[16,19–22], while stabilizing HIF-1α can increase Mtb control[17,23,24]. There are several compounds available that can modify HIF-1α expression in different ways. Deferoxamine (DFO), an iron chelator that inactivates PHD and FIH (**Fig. 1B**), and dimethyloxalylglycine (DMOG), an inhibitor of PHD (**Fig. 1B**), are examples of HIF-1α stabilizers[19,24]. KC7F2, a selective inhibitor of HIF-1α protein translation, is an example of a HIF-1α blocker[25].

While HIF-1α expression in macrophages seems beneficial for Mtb control, a thorough understanding of its effect on macrophage phenotype is not yet achieved. In this project, an *in vitro* model of Mtb infection of human blood-derived macrophages was employed to determine the effect of infection on expression of functional and phenotypical macrophage markers as well as M1/M2 polarization, in addition to how this is influenced by HIF-1α stabilization and

blockade. While western blot (WB) is a common technique to detect and quantify HIF-1α expression, flow cytometry was used in this project to enable detection of HIF-1α in human macrophages.

Materials and Methods

Reagents

The HIF-1α stabilizers deferoxamine (DFO) mesylate salt and dimethyloxalylglycine (DMOG) as well as the HIF-1α blocker KC7F2 were obtained from Merck and used at indicated concentrations.

Bacterial strains

Two avirulent mycobacteria strains were used, BCG and H37Ra. BCG is an attenuated mycobacterial strain originating from *M. bovis* that is currently also the only vaccine approved to prevent TB[3]. H37Ra is an avirulent relative of the standard virulent Mtb lab strain H37Rv. It contains several genetic modifications compared to H37Rv that altogether affect e.g. substrates of the type VII secretion system of Mtb, stress response, lipid biosynthesis and energy metabolism[26]. In this project, BCG and H37Ra carrying a pFPV2 plasmid containing a green-fluorescent protein (GFP) gene and kanamycin resistance gene (BCG-GFP and H37Ra-GFP) were used to visualize green-labeled bacteria with flow cytometry.

Monocyte isolation and differentiation

Peripheral blood mononuclear cells (PBMCs) from healthy donors (Karolinska Hospital Blood Bank, Stockholm, Sweden) were isolated from buffy coat blood by density gradient centrifugation over Lymphoprep (GE Healthcare Life Sciences). $10x10^6$ PBMCs were added per well of a 6-well plate or $5x10^6$ PBMCs per well of a 12-well plate (tissue-treated culture plates, Nunc) and monocytes were allowed to adhere for 2-3 hours at 37°C in serum-free medium (RPMI 1640 (Sigma or Gibco), supplemented with 2 mM L-glutamine (Cytiva), 1 mM sodium pyruvate (Sigma) and 10 mM HEPES (Cytiva)). The non-adherent cells were removed by washing with serum-free medium. The remaining adherent monocytes (estimated at $1x10^6$ per well for 6-well plate and $0.5x10^6$ for 12-well plate) were differentiated to M0 macrophages by culturing for 7 days in complete medium (RPMI 1640, supplemented with 2 mM L-glutamine, 1 mM sodium pyruvate, 10 mM HEPES and 10% fetal bovine serum (FBS) (Merck)) supplemented with 50 ng/mL recombinant human Macrophage Colony-Stimulating Factor (M-CSF) (Peprotech).

Bacteria culture and infection of monocyte-derived macrophages

BCG-GFP and H37Ra-GFP were cultured in Middlebrook 7H9 medium, supplemented with 10% glycerol (only for H37Ra culture), 10% Oleic Albumin Dextrose Catalase enrichment and 0.05% Tween-80 (Karolinska University Hospital Huddinge, Sweden) for 7-8 days. Bacterial suspensions were pelleted and washed with phosphate-buffered saline pH 7.4 (PBS) containing 0.05% Tween-80 and then resuspended in 5 mL of serum-free medium. After 5 min pulse-sonication to disrupt bacterial clumps, the optical density (OD) was measured at 600 nm. The number of colony-forming units (CFU) was calculated using the following formula: $(OD+0.155)/0.161 * 10^7$ = number of CFU/mL. The final bacterial concentration was adjusted appropriately by adding serum-free medium.

After 7 days of monocyte culture as described before, the human MDMs were infected with BCG-GFP or H37Ra-GFP for 4 hours at 37°C at a multiplicity of infection (MOI) of 1 or 5. For all HIF-1α experiments, BCG-GFP at MOI:5 was used. Afterwards, the cells were washed with PBS-0,05% Tween-80 to remove extracellular bacteria and subsequently cultured in RPMI complete medium, untreated or supplemented with DFO, DMOG or KC7F2 in various concentrations, until analysis.

Flow cytometry

BCG/H37Ra-infected and non-infected MDMs were detached at 24 hours post-infection using FACS buffer (PBS supplemented with 2 mM EDTA and 5% FBS) for 45 min at 37°C. Cells were

washed again with FACS buffer and subsequently surface markers were stained for 20 min at room temperature (RT). Fixation and permeabilization was done using eBioscience™ Foxp3/Transcription Factor Staining Buffer Set (Invitrogen). Intracellular staining was done for 30 min at RT. Finally, cells were washed and resuspended in FACS buffer. Cells were acquired using an LSR Fortessa instrument (BD Biosciences) controlled by FACSDiva software (BD Biosciences) and analyzed using FlowJo v10.8. BCG-GFP and H37Ra-GFP expression were visualized in the FITC channel. LIVE/DEAD™ Fixable Aqua Dead Cell Stain Kit (Life Technologies) was used to visualize live and dead cells. An overview of used antibodies and function of the macrophage markers is shown in **Table 1**. When evaluating single marker expression, the mean fluorescent intensity (MFI) of that marker within the live cell population was used, corrected for the MFI of the unstained control of the same sample to remove the effect of autofluorescence.

Table 1. Antibodies used for flow cytometry.

Target	Function	Fluorochrome	Clone	Company	Dilution
CCR7	Chemokine receptor	BV711	G043H7	BioLegend	1:50
CD163	Scavenger receptor	BV421	GHI/61	BioLegend	1:25
CD200R	CD200 glycoprotein receptor	PE	OX-108	BioLegend	1:50
CD206	Mannose receptor	APC-Cy7	15.2	BioLegend	1:25
CD40	TNF-α receptor	PE-Cy5	5C3	BD Biosciences	1:50
CD64	IgG receptor	PE DAZZLE 594	10.1	BioLegend	1:50
CD80	Co-stimulatory molecule	BV650	2D10	BioLegend	1:50
CD86	Co-stimulatory molecule	BV785	IT2.2	BioLegend	1:50
HIF-1α	Transcriptional regulator	AF647	546-16	BioLegend	1:25
HLA-DR	Antigen presentation	PE-Cy7	L243	BioLegend	1:50
IDO	Immune inhibitory enzyme	AF700	eyedio	Thermo Fisher	1:50
PD-L1	Immune checkpoint molecule	BV605	29E.2A3	BioLegend	1:25
TLR2	Pathogen-sensing receptor	AF647	TL2.1	BioLegend	1:50

Quantitative real-time PCR

RNA was extracted from uninfected or BCG-infected MDMs 24 hours post-infection using Ribopure RNA extraction kit as described by the manufacturer (Ambion, Thermo Fisher Scientific). cDNA was synthesized using Super Script Vilo™ cDNA Synthesis Kit (Thermo Fisher Scientific). Transcripts of IL-1β, CAMP and HIF-1α (primers obtained from Thermo Fisher Scientific) were measured in duplicates relative to the housekeeping gene 18S rRNA (eukaryotic 18S rRNA-housekeeping gene kit, Life Technologies), using quantitative real-time PCR (RT-PCR) (QuantStudio 5 Real-Time PCR System, Thermo Fisher Scientific). The relative amount of target mRNA was calculated using the $2^{-(\Delta\Delta Ct)}$ method. Data are presented as fold change of mRNA relative to uninfected and untreated MDMs.

Western blot

MDMs were lysed with RIPA buffer (Sigma) and total protein lysates were separated by SDS-PAGE using 4-12% pre-cast gradient gels (Invitrogen). The gels were blotted on a nitrocellulose membrane (Trans-blot Turbo Transfer mini; Biorad), followed by blocking for one hour with 5% milk in Tris-buffered saline-0,05% Tween-80 (TBS-T) at RT. Primary staining was

done with anti-HIF-1α (BD Biosciences; 1:500) and anti-tubulin (Cell signaling; 1:2000) overnight at 4°C. After washing with TBS-T, secondary staining was done with rabbit-anti-mouse-horseradish peroxidase (HRP) (GeneTex; 1:1000) and goat-anti-rabbit-HRP (Abcam; 1:2000), for HIF-1α and tubulin respectively, for one hour at RT. After washing, blots were treated with Clarity or Clarity Max ECL western blotting substrate (Biorad) and then developed and imaged with a ChemiDoc MP system (Biorad). Normalization of HIF-1α bands to the tubulin bands was not possible due to the high background signal in the HIF-1α images.

Statistical analysis

Statistical analysis was performed using Excel 2016 software. For the experiments regarding HIF-1α, several similar experiments were performed with different donors. As they differed in the conditions or treatments of the cells (uninfected/infected conditions and DFO/DMOG/KC7F2 concentrations), these experiments are presented separately. Only for the experiments including the full macrophage panel and one experiment with HIF-1α, two donors are presented simultaneously by showing mean ± range. Significant differences could not be determined as a minimum of three donors is required to perform non-parametric statistical tests.

Results

M1 and M2 polarization of uninfected and mycobacteria-infected macrophages

At 24 hours post-infection with BCG or H37Ra, morphology of the MDMs was studied using light microscopy. Uninfected macrophages were small and demonstrated a stretched morphology (**Fig. 2A**), while macrophages infected with BCG or H37Ra at MOI:1 were larger and more rounded but some maintained a stretched appearance (**Fig. 2B,D**). At MOI:5, the stretched morphology was lost almost completely as compared to MOI:1. Instead, macrophages were large, round, and more granular (**Fig. 2C,E**). There is no clear difference in morphology between macrophages infected with BCG or H37Ra at the same MOI.

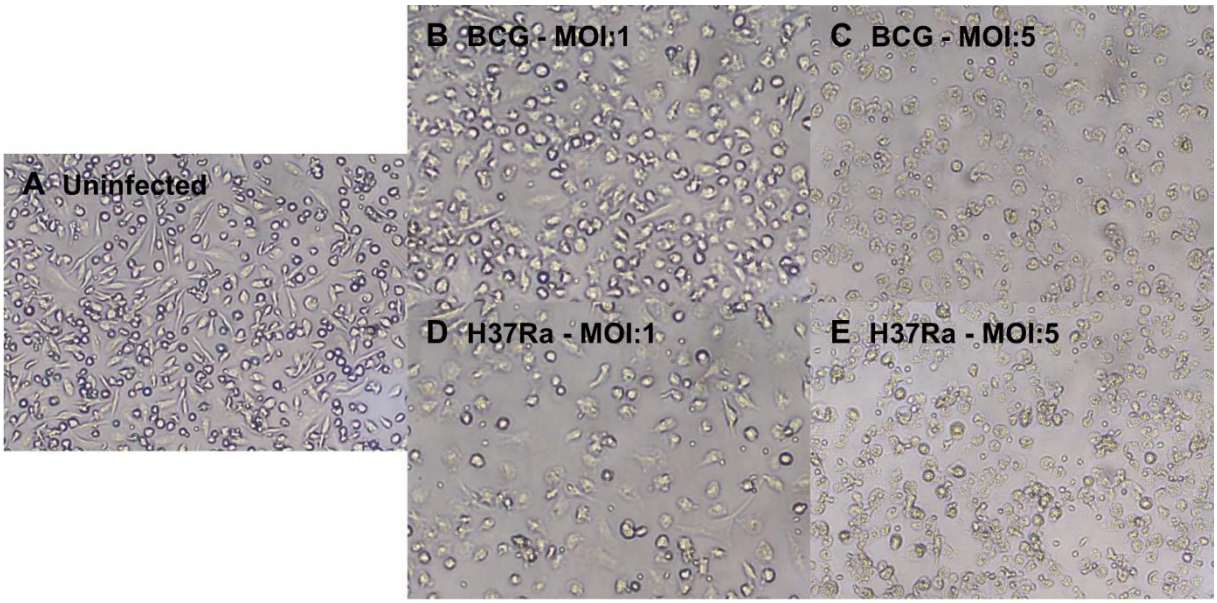

Figure 2. Morphology of uninfected and infected MDMs. *Microscopy pictures of (A) uninfected, BCG-infected at (B) MOI:1 and (C) MOI:5, and H37Ra-infected at (D) MOI:1 and (E) MOI:5. All pictures were taken at 24 hours post-infection with 10x magnification.*

Next, the phenotype of uninfected, BCG- or H37Ra-infected macrophages was studied using flow cytometry and a panel of surface markers (one intracellular) depicted in **Table 1**. The gating strategy employed can be viewed in **Supp. Fig. 1**. Viability of the macrophages was not markedly affected by infection with these avirulent strains (**Fig. 3A**). The percentage of productively infected macrophages differed substantially between BCG and H37Ra, both at MOI:1 (1% vs 9%) and MOI:5 (3% vs 29%) (**Fig. 3B**). These results suggested that H37Ra was more successful in infecting MDMs compared to BCG.

Two gating methods were used to study the macrophage polarization towards inflammatory M1 and anti-inflammatory M2 phenotypes. Method 1 was based on macrophages constitutively expressing CD64[27], while CD163 is primarily expressed on M2-polarized macrophages[8]. Accordingly, within the live cell population M1 macrophages were defined as CD64+CD163-, while M2 macrophages were defined as CD64+CD163+. When using this method, uninfected macrophages had an M2 phenotype of almost 100%, while in MOI:5 infected conditions there were more macrophages with an M1 than an M2 phenotype (approximately 30% vs 20%) (**Fig. 3C-D**). The loss of either the M1 or M2 phenotype can be explained by the increased proportion of macrophages that were CD64- (see **Supp. Fig. 1** for example). With method 2, M1 macrophages were defined as CD86+CD64+ within the live cell population, while M2 macrophages were defined as CD200R+CD163+[8]. Interestingly, both M1 and M2 were nearly 100% in the uninfected condition, indicating that most macrophages expressed both the selected M1 and M2 markers (**Fig. 3E-F**). At MOI:1 infection, the CD86+CD64+ M1 phenotype

decreased, and this trend continued at MOI:5 (**Fig. 3E**). The frequency of CD200R+CD163+ M2 cells was maintained at MOI:1 but was greatly decreased at MOI:5 (**Fig. 3F**). As a result, the M2 phenotype dominated with mild infection, while overt infection promoted a shift towards a more dominant M1 phenotype. Despite a difference in the proportion of Mtb-infected cells, H37Ra and BCG strains displayed similar effects on M1/M2 polarization (**Fig. 3C-F**).

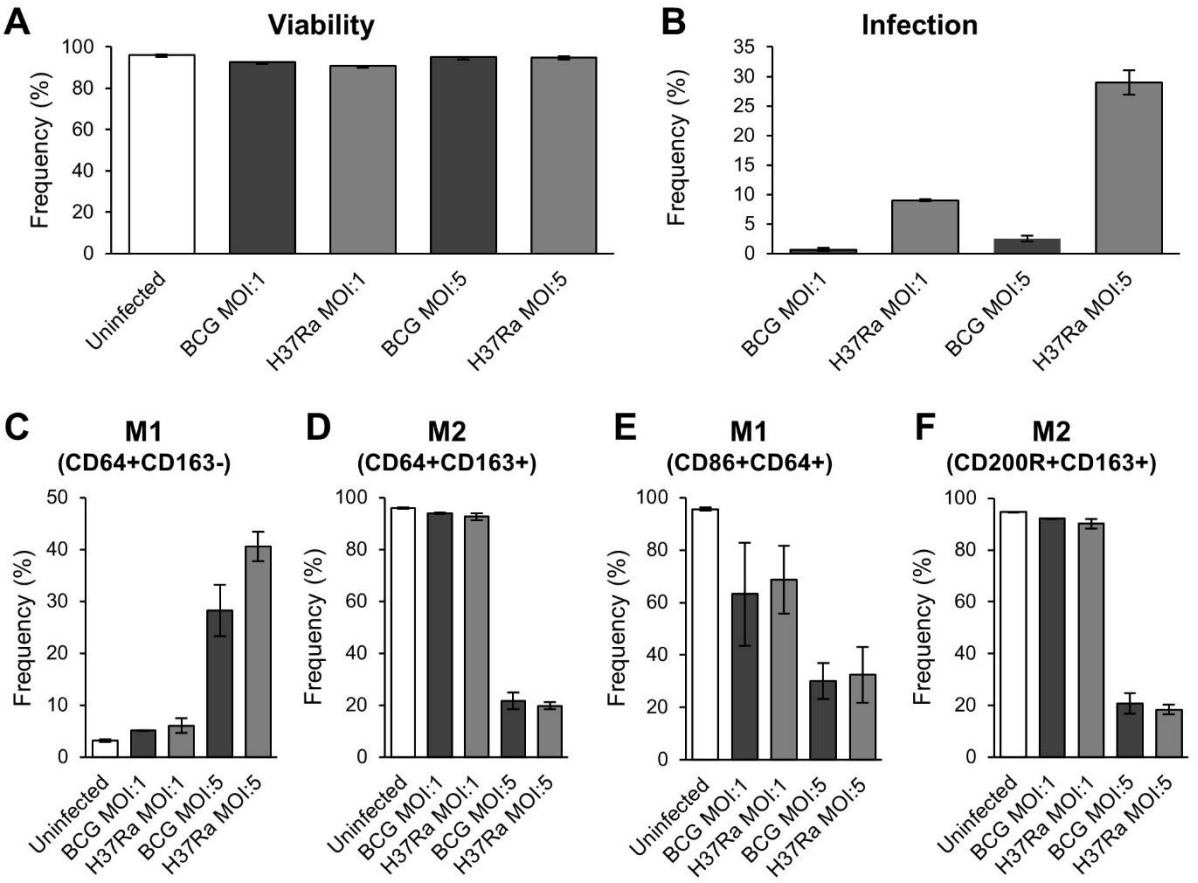

Figure 3. Phenotype of uninfected, BCG- and H37Ra-infected MDMs. *A) Percentage of viable cells. B) Percentage of infected cells within viable cells. C-D) Percentages of M1 (C) and M2 (D) phenotypes within viable cells as determined using method 1, where M1 cells were defined as CD64+CD163- and M2 cells as CD64+CD163+. E-F) Percentages of M1 (E) and M2 (F) phenotypes within viable cells as determined using method 2, where M1 cells were defined as CD86+CD64+ and M2 cells as CD200R+CD163+. Results were obtained from n=2 donors. Data is presented as mean ± range.*

Additionally, the difference in M1/M2 polarization between uninfected and infected cells within the same sample was studied for the H37Ra-infected macrophages only, as infection of macrophages with BCG was very limited. H37Ra-GFP-positive macrophages demonstrated a higher frequency of M1-polarized macrophages, while the frequency of M2-polarized macrophages was slightly lower compared to H37Ra-GFP-negative macrophages for both M1/M2 gating strategies (**Fig. 4**). However, the changes in M1- and M2-polarization when comparing MOI:5 to MOI:1 occurred in both H37Ra-GFP-positive and -negative macrophages (**Fig. 4**).

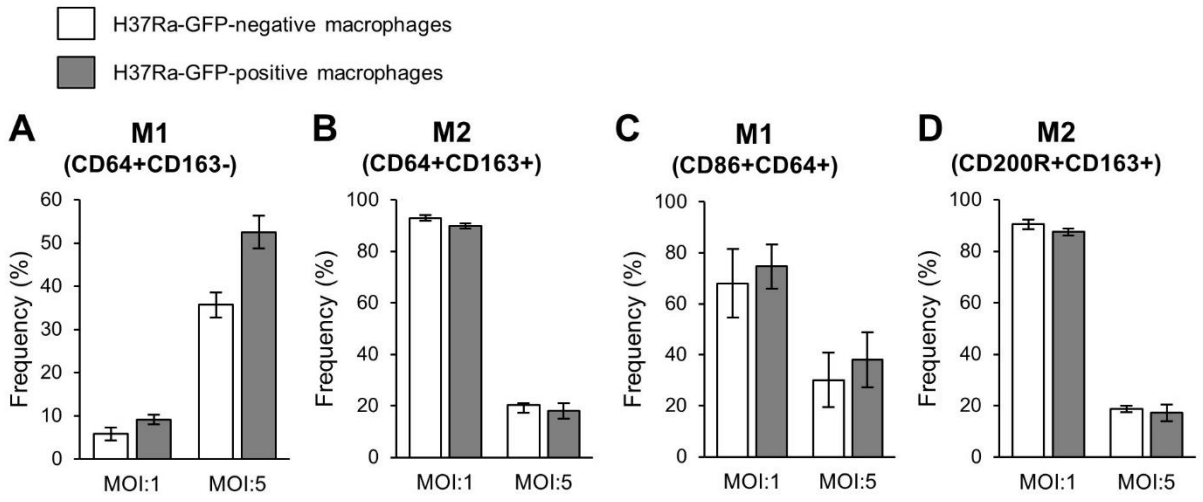

Figure 4. M1- and M2-polarization of H37Ra-GFP-negative and -positive macrophages. *Flow cytometry was used to determine the M1 and M2 phenotype of H37Ra-GFP-negative (uninfected) and H37Ra-GFP-positive (infected) macrophages within the MOI:1 and MOI:5 H37Ra-infected conditions. A-B) Percentages of M1 (A) and M2 (B) phenotypes within viable cells as determined using method 1, where M1 cells were defined as CD64+CD163- and M2 cells as CD64+CD163+. C-D) Percentages of M1 (C) and M2 (D) phenotypes within viable cells as determined using method 2, where M1 cells were defined as CD86+CD64+ and M2 cells as CD200R+CD163+. Results were obtained from n=2 donors. Data is presented as mean ± range.*

Expression of immune markers on uninfected and mycobacteria-infected macrophages

Toll-like Receptor 2 (TLR2), CD64 and C-C Chemokine Receptor type 7 (CCR7) are associated with inflammation and thus considered to be typical M1 markers. CCR7 increased markedly upon infection with BCG or H37Ra, while TLR2 and CD64 were increased at MOI:1 but declined to levels comparable to the uninfected control at MOI:5 (**Fig. 5A-C**). A similar expression pattern was observed for the M2 marker CD206, while the other M2 markers CD200 Receptor (CD200R) and CD163[10] were comparable to the uninfected control at MOI:1, but decreased dramatically at MOI:5 (**Fig. 5D-F**). The co-stimulatory molecule CD80 was highly increased at MOI:1 and remained higher compared to the uninfected control at MOI:5, while CD86 gradually decreased with a higher MOI (**Fig. 5G-H**). The expression of the antigen-presenting molecule HLA-DR was stable and similar to the uninfected control in all conditions (**Fig. 5I**). The pro-inflammatory marker CD40 (TNF-α receptor) was increased at MOI:1 and returned to baseline at MOI:5 (**Fig. 5J**). The immune checkpoint molecule Programmed Death-Ligand 1 (PD-L1) and the immune inhibitory enzyme Indoleamine 2,3-Dioxygenase (IDO) were both increased after infection at MOI:1 and 5 (**Fig. 5K-L**). Altogether, these results suggested that M1 markers were either stable or upregulated upon mycobacteria infection, while M2 markers were markedly downregulated apart from CD206, which combined is in agreement with the shift in M1/M2 polarization as observed before.

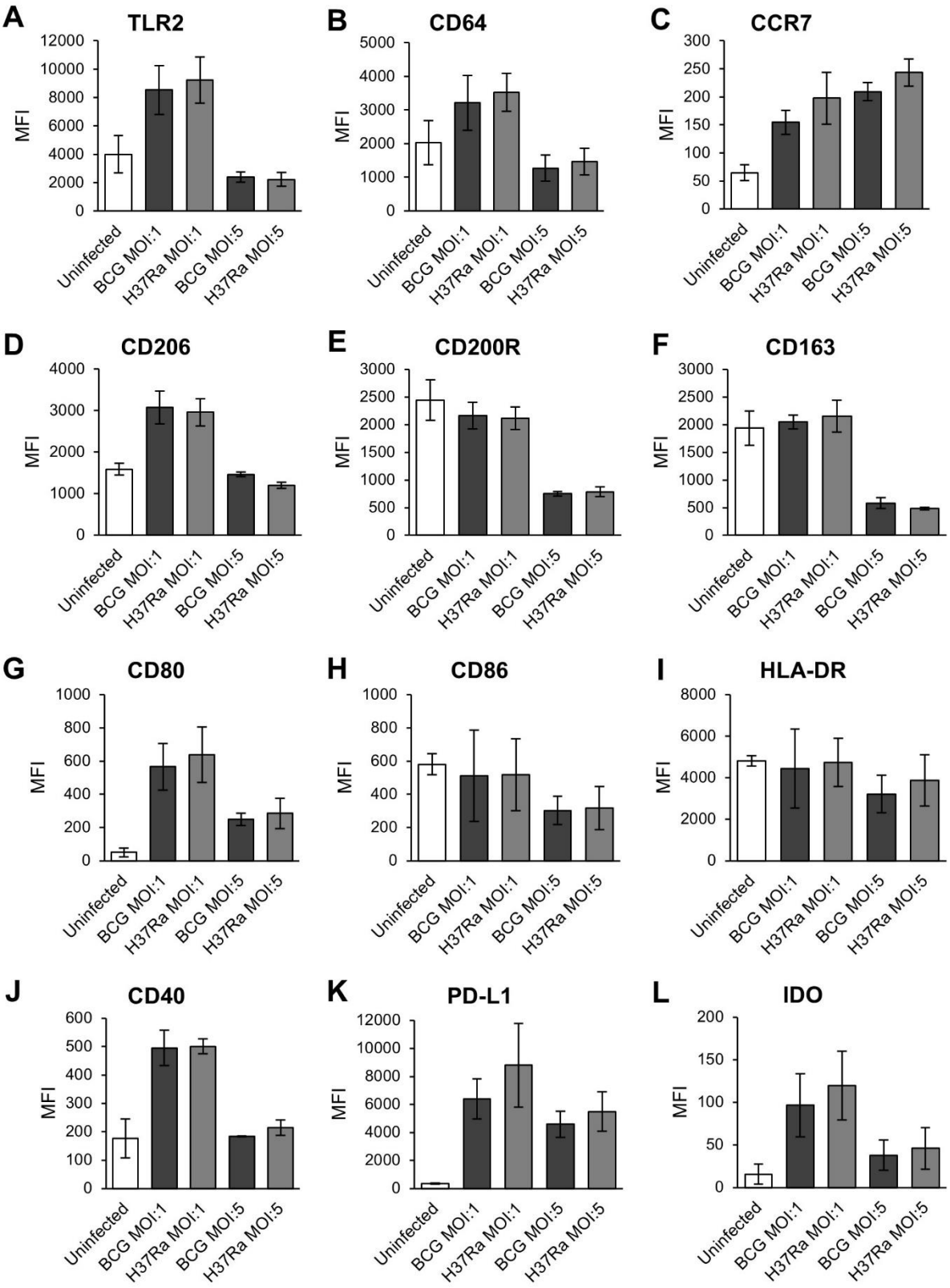

Figure 5. Expression of macrophage markers on uninfected, BCG- and H37Ra-infected MDMs. *Expression of M1 markers TLR2 (A), CD64 (B) and CCR7 (C), M2 markers CD206 (D), CD200R (E) and CD163 (F), co-stimulatory molecules CD80 (G) and CD86 (H), antigen-presenting molecule HLA-DR (I), pro-inflammatory marker CD40 (J), and immune checkpoint molecules PD-L1 (K) and IDO (L) within viable cells. Results were obtained from n=2 donors. Data is presented as mean ± range. Mean fluorescent intensity (MFI) was corrected for the background signal in the unstained control.*

Effects of HIF-1α modulators on HIF-1α expression and macrophage function

HIF-1α may regulate the transcriptional response of different immune cells including macrophages upon infection with Mtb[17,23,24,28,29]. While HIF-1α protein is normally detected using western blot, it was investigated here if HIF-1α could be detected using flow cytometry of mycobacteria-infected MDMs. For this purpose, two chemical HIF-1α stabilizers, DFO and DMOG, and one HIF-1α blocker, KC7F2, were used.

First, uninfected MDMs were treated with various concentrations of the HIF-1α stabilizers DFO and DMOG for 24 hours to determine potential toxicity and expression of HIF-1α using flow cytometry. The treatments did not affect viability, except for DMOG at a concentration of 1000μM (**Fig. 6A**). Next, the expression of HIF-1α was measured and quantified as the MFI in the fluorescent channel for HIF-1α (**Fig 6B**). An increased HIF-1α expression upon culture with the stabilizers could not be detected using flow cytometry (**Fig. 6C**). Although DMOG treatment seemed to increase the frequency of HIF-1α-positive cells slightly, the MFI was not increased (**Fig. 6B**). The HIF-1α-stabilizing effect of DFO and DMOG could also not be demonstrated at the mRNA level using quantitative RT-PCR (**Fig. 6D**).

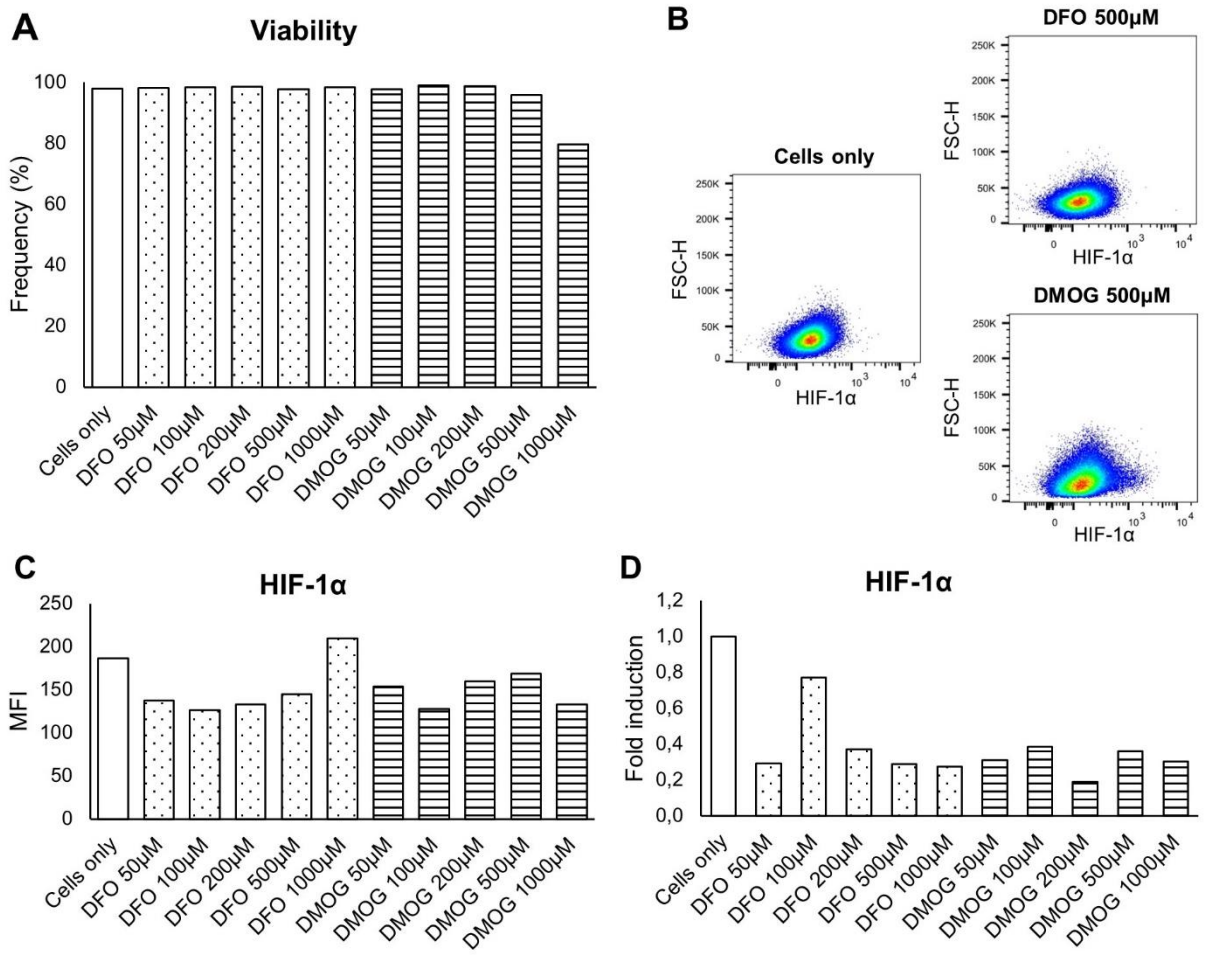

Figure 6. Viability and HIF-1α expression in uninfected MDMs treated with HIF-1α stabilizers DFO and DMOG*. A) Percentage of viable cells. B) Representative dot plots of FSC-HxHIF-1α within viable cells. C) MFI of HIF-1α within viable cells as determined with flow cytometry. D) Expression of HIF-1α mRNA as determined with RT-PCR, presented as fold change compared to untreated MDMs. Results were obtained from n=1 donor. Mean fluorescent intensity (MFI) was corrected for the background signal in the unstained control.*

For the continued experiments, 100µM and 500µM DFO and DMOG were chosen. BCG-infected macrophages were treated with DFO, DMOG or KC7F2 for 24 hours post-infection and compared to uninfected and untreated macrophages. HIF-1α expression was determined using flow cytometry (**Fig. 7A**). Infected macrophages showed a relatively lower MFI of HIF-1α expression compared to uninfected macrophages (**Fig. 7B**). As expected, DFO seemed to induce a concentration-dependent increase in HIF-1α expression, while a concentration-dependent decrease was observed for KC7F2-treated conditions (**Fig. 7B**). However, DMOG did not induce an increase of HIF-1α MFI (**Fig. 7B**). RT-PCR was also unsuccessful in demonstrating an effect of the compounds on HIF-1α mRNA expression (**Fig. 7C**). Next, RT-PCR was used to study the effect of DFO, DMOG and KC7F2 on the expression of the pro-inflammatory cytokine IL-1β and Cathelicidin Antimicrobial Peptide (CAMP; also known as LL-37 in its active form). IL-1β was slightly induced in the infected macrophages compared to the uninfected control (**Fig. 7D**). In addition, an even stronger and dose-dependent increase was visible after treatment of BCG-infected cells with DFO and DMOG, while KC7F2 decreased IL-1β expression (**Fig. 7D**). CAMP expression was already low in the uninfected control and declined further after BCG-infection (**Fig. 7E**). The effects of the chemical compounds on CAMP expression were unclear (**Fig. 7E**).

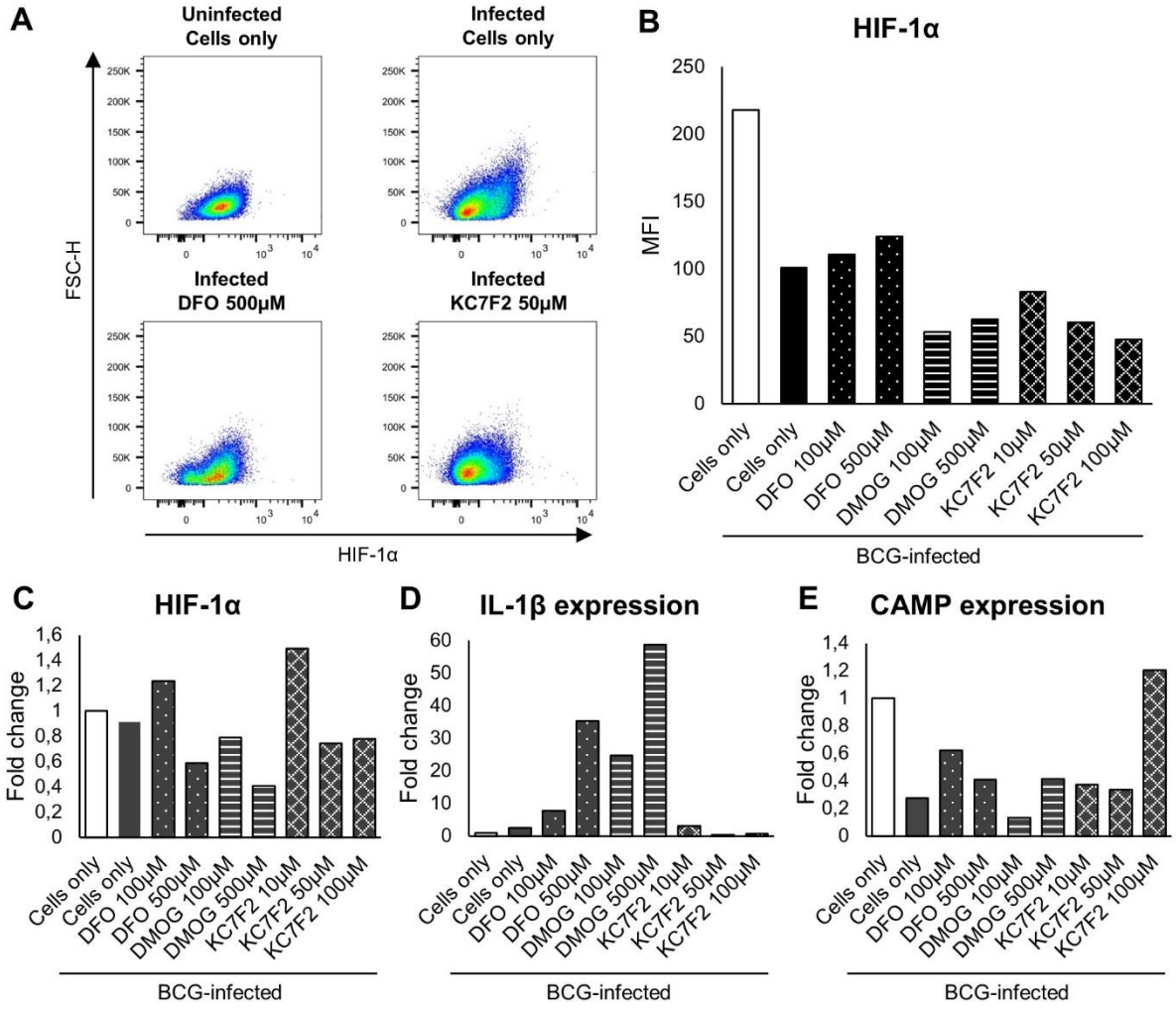

Figure 7. Expression of HIF-1α and macrophage effector molecules in BCG-infected MDMs treated with the HIF-1α stabilizers DFO and DMOG and the HIF-1α blocker KC7F2. *A) Representative dot plots of FSC-HxHIF-1α within viable cells. B) MFI of HIF-1α within viable cells as determined with flow cytometry. C-E) Expression of (C) HIF-1α, (D) IL-1β and (E) CAMP (LL-37) mRNA as determined with RT-PCR, presented as fold change of each target gene compared to untreated and uninfected MDMs. Results were obtained from n=1 donor. Mean fluorescent intensity (MFI) was corrected for the background signal in the unstained control.*

In a separate experiment, DFO, DMOG and KC7F2 were tested in both uninfected and BCG-infected MDM cultures from two donors and HIF-1α expression was determined using flow cytometry (**Fig. 8A**). In uninfected macrophages, treatment with DFO or DMOG seemed to increase HIF-1α MFI, while a decrease with KC7F2 could not be observed (**Fig. 8B**). In BCG-infected macrophages, DFO seemed to increase HIF-1α MFI, but DMOG- and KC7F2-treated conditions were roughly similar to untreated infected cells (**Fig. 8B**). Infection of MDMs seemed slightly reduced in the presence of DFO as well as KC7F2 (**Fig. 8C**). M1/M2 polarization was studied with gating method 1, as described previously (see **Supp. Fig. 1** for example). As seen before, uninfected conditions displayed a low frequency of M1 cells that was increased after infection (**Fig. 8D**), while M2 polarization demonstrated the opposite relationship (**Fig. 8E**). Neither M1 nor M2 polarization seemed to be affected by the HIF-1α modulators, with the exception of one outlier in DMOG-treated uninfected macrophages (**Fig. 8D-E**).

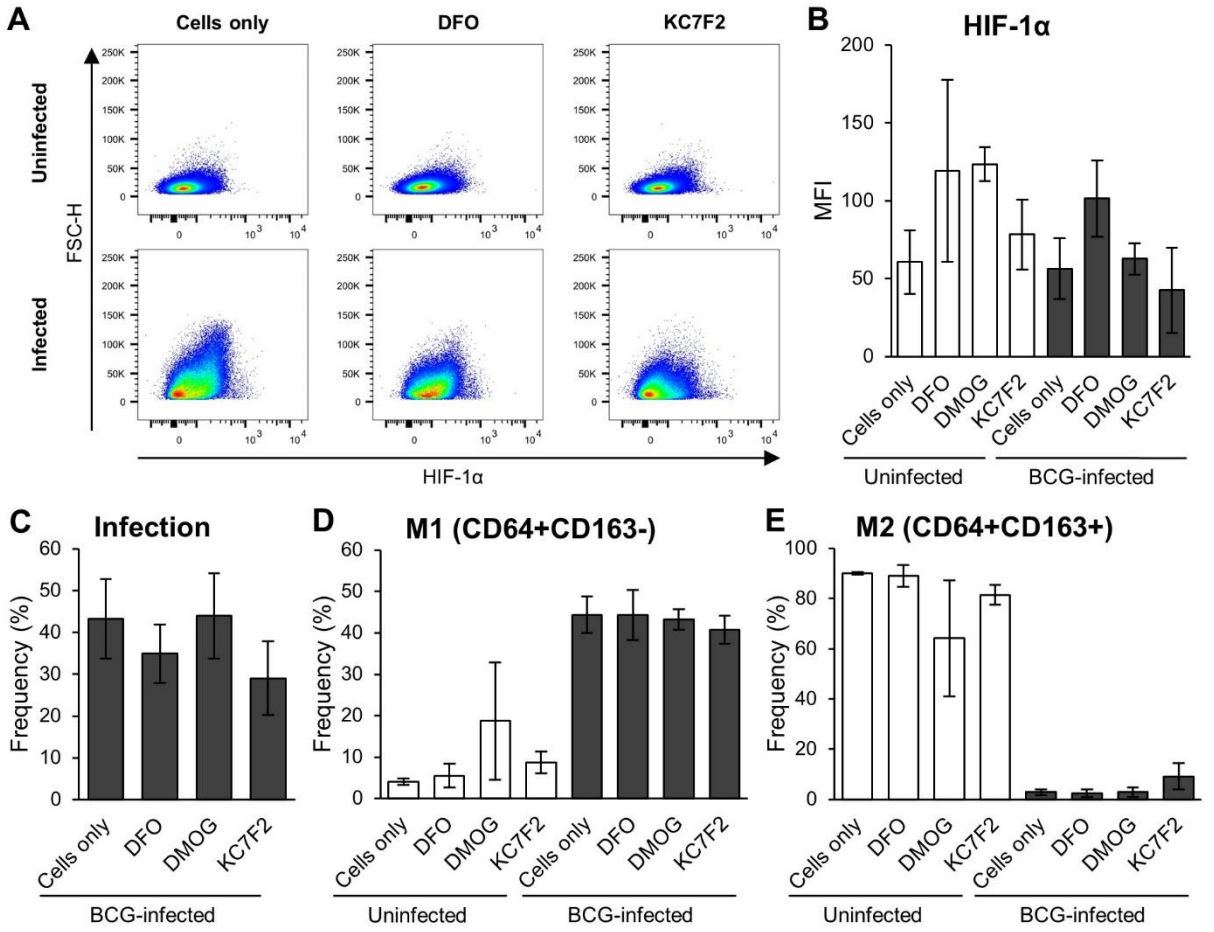

Figure 8. HIF-1α expression and M1/M2 polarization in uninfected and BCG-infected MDMs treated with the HIF-1α stabilizers DFO and DMOG and the HIF-1α blocker KC7F2. *Concentrations used were 500μM for DFO and DMOG and 25μM for KC7F2. A) Representative dot plots of FSC-HxHIF-1α within viable cells from one donor. B) MFI of HIF-1α and C) percentage of BCG-infected cells within viable cells as determined with flow cytometry. D-E) Percentages of M1 (D) and M2 (E) phenotypes within viable cells as determined using method 1, where M1 cells were gated as being CD64+CD163- and M2 cells as CD64+CD163+. Results were obtained from n=2 donors. Data is presented as mean ± range. Mean fluorescent intensity (MFI) was corrected for the background signal in the unstained control.*

As the chemical compounds did not consistently demonstrate the expected effect on HIF-1α expression when measured with flow cytometry, this method was compared to WB, which is the conventional method to determine HIF-1α protein expression. Two different donors were tested and the results of HIF-1α flow cytometry were compared to WB for each individual donor A (**Fig. 9A**) and B (**Fig. 9B**). For donor A, a dose-dependent increase in HIF-1α expression could be observed with WB after DFO treatment in both uninfected and BCG-infected macrophages, as well as for DMOG in BCG-infected macrophages (**Fig. 9A**). Additionally, HIF-1α expression was higher for uninfected macrophages compared to infected macrophages (**Fig. 9A**). These results were in line with the MFI of HIF-1α as measured with flow cytometry, although the differences between the conditions were not as strong as with WB and with the exception of uninfected macrophages treated with 100μM DFO (**Fig. 9A**). For donor B, a dose-dependent increase in HIF-1α expression was observed after DFO treatment with WB in both uninfected and BCG-infected macrophages, but with a stronger effect in uninfected macrophages (**Fig. 9B**). Unlike donor A, uninfected and BCG-infected untreated macrophages both demonstrated low HIF-1α expression (**Fig. 9B**). These effects could not be visualized with flow cytometry, as there was no concentration-dependent effect of DFO visible for either uninfected and BCG-infected cells and also the levels for untreated macrophages and uninfected DFO-treated macrophages did not correspond with the WB results (**Fig. 9B**). As HIF-1α expression was already very low in BCG-infected and untreated cells, the effect of HIF-1α blocker KC7F2 could not be demonstrated with WB (**Fig. 9**).

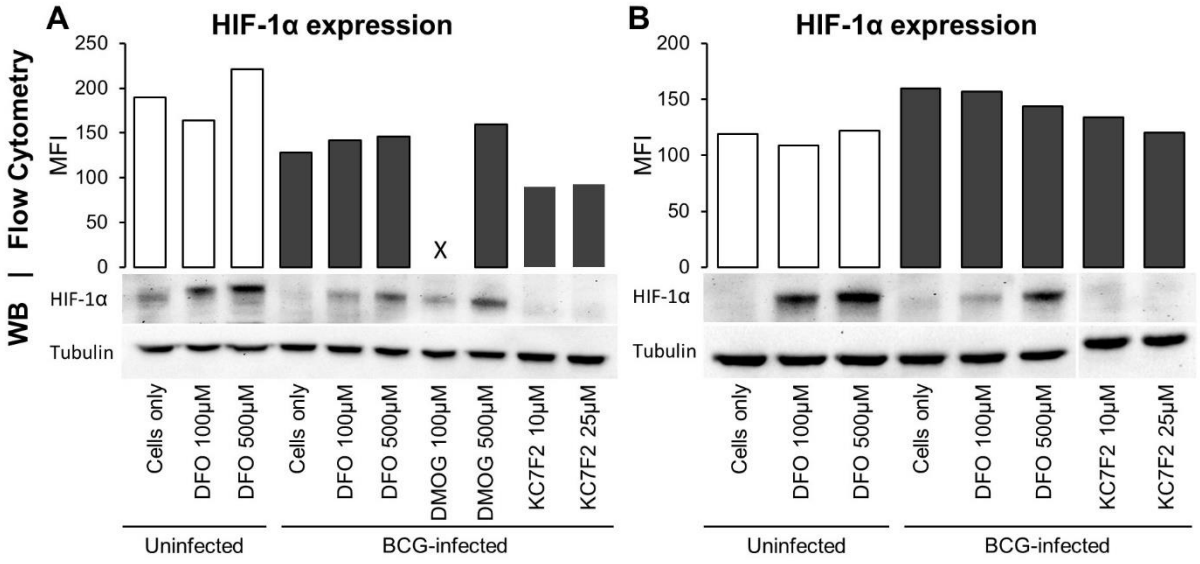

Figure 9. Comparison of flow cytometry and WB to measure HIF-1α expression in uninfected and BCG-infected macrophages treated with DFO, DMOG or KC7F2. *A and B represent the results of two different donors. In A) the MFI for DMOG 100μM treatment is missing due to an experimental error. Mean fluorescent intensity (MFI) was corrected for the background signal in the unstained control. Tubulin was used as a loading control for WB.*

Discussion

In this project, an *in vitro* infection model for Mtb was employed to study the changes in functional and phenotypical markers as well as M1/M2 polarization of MDMs after infection with different Mtb stains and after manipulation of HIF-1α expression. Uninfected MDMs showed a strong M2 phenotype, but this decreased after infection with BCG or H37Ra at a higher MOI. Depending on the gating method used, the M1 phenotype increased or decreased with infection, but importantly both gating methods demonstrated that the final M1/M2 ratio was skewed slightly in favor of the M1 phenotype after BCG or H37Ra infection at MOI:5. In addition, H37Ra-infected cells exhibited a slightly higher frequency of M1 cells, while the frequency of M2 cells was slightly lower compared to uninfected cells within the same sample, supporting the notion that infection skews macrophage phenotype. Likewise, analyses of expression of individual M1 and M2 markers suggested that M1 markers and the pro-inflammatory marker CD40 were generally either stable or upregulated after infection at higher MOI, while M2 markers were either stable or downregulated, which also suggests an Mtb-induced shift towards the M1 phenotype. All in all, the skewing towards the M1 phenotype is favorable for combating Mtb infection.

The observation that uninfected MDMs differentiated with M-CSF have a prominent M2 phenotype is in line with findings from Rao Muvva[10]. Here, it was also observed that distinct M1 or M2 polarization were shifted to a mixed M1/M2 phenotype at 4 hours post-infection with H37Rv, while this effect was less clear at 24 hours post-infection[10]. However, considering that BCG and H37Ra are less virulent than H37Ra, the mixed M1/M2 phenotype observed here at 24 hours post-infection can take longer to manifest than for H37Rv. The observed increase in PD-L1 and IDO expression with BCG- and H37Ra-infection may counteract the pro-inflammatory and antibacterial effect of M1 polarization of macrophages. The immunosuppressive myeloid region of TB granulomas, where Mtb presence is maintained, has been shown to be characterized by increased expression of both PD-L1 and IDO[30,31]. Thus, these immune inhibitory molecules could be promising targets for adjunct therapy of TB. Interestingly, activated T cells in the TB granuloma hardly expressed PD-1[30], suggesting that potential repurposing of anti-PD-L1 antibody therapy for cancer might be more successful than anti-PD-1 therapy. However, reactivation of latent TB has been observed in cancer patients treated with PD-1 blockade, and more rarely with PD-L1 blockade, indicating that more research into their effect on TB is needed[32,33].

Next, the effect of HIF-1α expression on macrophage M1/M2 polarization and functionality during Mtb infection was studied. Several other studies have investigated the role of HIF-1α expression in macrophages infected with Mtb. Interferon-γ (IFN-γ) produced by CD4+ T cells is an important factor in TB control as it induces macrophage activation[9]. When HIF-1α$^{-/-}$ BMDMs are used in an *in vitro* infection model, IFN-γ-dependent control of Mtb growth is reduced compared to wild-type (WT)[16,19]. In addition, in HIF-1α$^{-/-}$ BMDMs many inflammatory cytokines and chemokines as well as NO are produced less compared to WT IFN-γ-stimulated BMDMs[19]. The reduction of NO when HIF-1α expression is reduced corresponds with the idea that HIF-1α and iNOS are linked in a positive feedback loop[20]. NO is crucial for the killing capacity of macrophages but also inhibits NF-kB activity to prevent pathological inflammation[20]. CD4+ T cells can also mediate Mtb control in macrophages in an IFN-γ-independent manner by activating macrophages and stimulating M1 polarization. This process is dependent on HIF-1α as well[21]. Moreover, HIF-1α is important for the activation of macrophages in response to Early Secreted Antigenic Target 6-kDa protein (ESAT-6). ESAT-6 is one of the major virulence factors of Mtb, but is also of interest in vaccine studies due to its immunogenicity[34]. THP-1 macrophages increase phagocytosis and production of ROS, as well as switch towards glycolysis, when treated with ESAT-6. These effects are reduced when HIF-

1α expression was blocked using small interfering RNA, indicating that HIF-1α plays at least a partial role in the protective activation of macrophages conferred by ESAT-6 exposure[22]. Stabilizing HIF-1α was shown to have the opposite effect of blocking HIF-1α, namely increase Mtb control in macrophages. Treating Mtb-infected U937 macrophages with $CoCl_2$ to activate HIF-1α results in enhanced autophagy, a physiological process important for the degradation of debris and intracellular pathogens like Mtb, and increased production of the pro-inflammatory cytokines TNF-α and IL-6[23,35]. Treatment with DFO can enhance glycolytic metabolism in both Mtb-infected and uninfected human MDMs, as well as stimulate IL-1β expression[24]. Next to this, the PHD-inhibitor Molidustat can induce a vitamin D-mediated antimicrobial pathway by upregulation of the vitamin D receptor and subsequent production of β defensin 2 in human MDMs infected with Mtb[17]. Ultimately, stabilization of HIF-1α seems to result in a reduction of intracellular Mtb growth in these *in vitro* infection models[17,23].

Here, we showed that the pro-inflammatory cytokine IL-1β was upregulated in BCG-infected conditions after treatment with HIF-1α stabilizers DFO and DMOG, in line with previous results[24], and potentially downregulated by the HIF-1α blocker KC7F2. These chemical modulators of HIF-1α did not impact expression of the antimicrobial peptide CAMP. A change in M1/M2 polarization by treatment with DFO, DMOG and KC7F2 could not be demonstrated, either in uninfected or BCG-infected conditions. In addition, the effectivity of flow cytometry to determine HIF-1α expression was evaluated. The effect of the HIF-1α modulators, as well as the effect of infection itself, on HIF-1α expression as measured via flow cytometry was highly variable over different experiments. Parallel WB experiments revealed that this method seems to be more sensitive and less subject to donor variation when determining HIF-1α expression compared to the currently used flow cytometry protocol. However, it might be possible to optimize the determination of HIF-1α expression via flow cytometry, perhaps by using a HIF-1α antibody in a different channel, changing the concentration of the antibody used or increasing the incubation time. Additionally, the blocking effect of KC7F2 still needs to be validated, which could for example be done by comparing simultaneous treatment with DFO and KC7F2 to only DFO treatment.

Although the effects of DFO, DMOG and KC7F2 could not be demonstrated consistently with flow cytometry, the WB experiments showed that at least DFO and DMOG were successful at enhancing HIF-1α expression. Additionally, DFO and DMOG have previously been used at concentrations of 100μM -200μM in MDMs or BMDMs[15,17,19,20,24,36] and their effect on HIF-1α has been confirmed with western blot[18,19,24]. Therefore, it is likely that DFO and DMOG were successful in stabilizing HIF-1α in all experiments. The effect of BCG-infection itself on HIF-1α expression was unclear from these experiments, as the WB showed a decrease for one donor and stable low expression in another. It has been reported that uninfected BMDMs and MDMs have low expression of HIF-1α, but although Mtb infection seems to increase HIF-1α expression, this effect might be variable and time-dependent as an increase could not always be observed after 24 hours of infection[16,18,19,24]. Next to time post-infection, these differences could also be attributed to e.g. donor variation and Mtb strain used. However, it has been shown that human pulmonary TB lesions are hypoxic and that macrophages within the granuloma express HIF-1α[18], suggesting that the *in vitro* Mtb infection model used here might not be fully representative concerning HIF-1α expression in relation to Mtb infection. Additionally, we were unable to demonstrate changes in HIF-1α with RT-PCR, while this has been successful in different studies[15–17]. The Ct values for HIF-1α obtained with RT-PCR, as well as for CAMP, were very high, indicating that very little cDNA of these genes was present, thus making detection less reliable. This could potentially have been improved by increasing the amount of cDNA added in the RT-PCR reaction, but this was not pursued further due to time constraints.

A strength of this study is the use of an established *in vitro* model for Mtb infection with human MDMs using a validated multi-color flow cytometry panel, so macrophage function and M1/M2 polarization could be studied in detail[8,10]. Additionally, flow cytometry and WB were directly compared to give more insight into the reliability of determining HIF-1α expression via the MFI measured with flow cytometry. However, there are also several limitations. Firstly, donor variation is substantial when working with human MDMs, for example related to efficacy of M0 differentiation with M-CSF or infectivity with Mtb. These can lead to large differences within the same experiment or different experiments, especially when maximum two donors are used like in this study. Therefore, this study should be repeated with more donors, at least three per experiment, in order to validate the present results or discover new results. Secondly, the MOI used with this protocol may not be very accurate, as plate adherence is used to isolate monocytes from PBMCs, so the number of monocytes per well will differ per donor and experiment. This could have been avoided by using a beads-based approach to isolate monocytes prior to cell seeding, but this method is significantly more expensive and time-consuming compared to plate-adherence. In addition, the accuracy of bacteria counting by measuring OD at 600 nm is not very high, especially for lower concentrations of bacteria that can be overestimated. A different counting method, e.g. the BactoBox, could improve accuracy. Thirdly, the autofluorescence of BCG- and H37Ra-infected cells at MOI:5 increases markedly and gives a broad spectrum in the channel used for the viability dye (**Supplementary Fig. 1B**). Therefore, when setting the gate for live cells based on the unstained control, it is possible that dead cells are partly included in the gating. This complicates comparing viability between uninfected and infected conditions. Additionally, this could have contributed to the lower increase of macrophage markers in MOI:5 compared to MOI:1 conditions, as dead cells would likely have lower expression of these markers. However, this was still considered the best gating strategy for live cells, as gating a smaller population may enhance purity, but simultaneously excludes productively infected cells with higher autofluorescence. All in all, for future experiments it would be better to use a different viability dye in a channel where this high autofluorescence is not observed. Lastly, gating and analysis of flow cytometry data is based on subjective interpretation. There is no uniform gating strategy to study M1/M2 polarization with flow cytometry. The two methods described here both have advantages and disadvantages. Method 1 (CD64+CD163- for M1 and CD64+CD163+ for M2) may be beneficial as gating on CD64+ cells ensures visualization of fully differentiated macrophages, since CD64 is constitutively expressed by macrophages[27]. In addition, this method divides the whole macrophage population as either M1 or M2. This helps to simplify the concept of M1/M2 polarization, but a disadvantage is that the spectrum between M1 and M2 polarization is lost. Method 2 is better at preserving this spectrum, as it shows whether the macrophages have M1 or M2 characteristics, where one does not exclude the other. However, while the M2 phenotype of CD200R+CD163+ seems reserved for M2 macrophages, it has been demonstrated that M2 macrophages can also be CD86+CD64+ although to a lower extent than M1[8]. This makes it more complicated to interpret the M1/M2 phenotype, but on the other hand is likely more in line with the *in vivo* situation where pure M1 or M2 populations are rare[6]. Furthermore, there are multiple options for the analysis of individual markers. In the present study it was chosen to determine MFI. Gating the percentage of positive cells might be another way to quantify expression. This method works best when the samples are uniform in the position of the positive population, which was not always the case for HIF-1α and the reason why MFI was chosen to measure HIF-1α expression.

Repeating current experiments with more donors is important to validate the results on M1/M2 phenotype after HIF-1α modulation of macrophages. Furthermore, transcriptional profiling including other macrophage effector molecules such as cytokines (e.g. TNF-α, IL-6, IL-10), autophagy markers (e.g. Beclin-1), immune regulatory factors (e.g. IDO and IL-1 receptor

antagonist), arginase-1 and inducible nitric oxide could be of importance[10]. In addition, co-culture models that include T cells or dendritic cells (DCs) combined with macrophages could be the next step for *in vitro* models more resembling of the *in vivo* situation. Contrary to the generally positive effect of HIF-1α stabilization in macrophages on Mtb defense, this might not be the case for T cells and DCs. Mice with a T cell-conditional knock-out of VHL, a negative regulator of HIF-1α (**Fig. 1B**), demonstrated a higher bacterial burden in the lungs and lower survival after Mtb infection compared to WT mice[28]. Additionally, there was less infiltration of Mtb-specific CD4+ T-cells into the lungs of these mice and the CD4+ T cells were less proliferative in combination with increased expression of inhibitory receptors PD-1 and cytotoxic T-lymphocyte-associated protein 4 (CTLA-4)[28]. These effects were abrogated in a conditional double knock-out of VHL and HIF-1α, indicating dependency on HIF-1α[28]. For DCs, it was shown that Mtb-infected macrophages secrete factors that induce DC maturation, but this process was counteracted when HIF-1α in DCs was stabilized either by DMOG or via a natural response when DCs were infected with Mtb[29]. Thus, it would be interesting to study the total effect of HIF-1α stabilization in co-cultures where the effect on macrophages is likely positive but for T cells or DCs the corresponding effect might be negative. An alternative model could be the use of an *in vitro* 3-dimensional granuloma model, e.g. described by Kotze *et al.* that uses alveolar macrophages from TB patients as well as lymphocytes taken from blood to build a spheroid lung granuloma model that resembles early innate and later adaptive stages of the human granuloma[37]. However, there is still much development and optimization of such models that could be challenging. Thus, experimental models such as mice can still be relevant to study the effects of HIF-1α modulation in an *in vivo* setting of Mtb infection. Mouse models have demonstrated an increase of HIF-1α expression in macrophages and T cells within granulomas and the switch towards glycolytic metabolism upon Mtb infection[16,38]. HIF-1α$^{-/-}$ mice (conditional deletion in the myeloid lineage) had higher bacterial loads in the lungs[19] and survival of HIF-1α$^{-/-}$ mice was dramatically decreased compared to WT mice in Mtb infection models[16,19]. Additionally, macrophages isolated from the lungs of Mtb-infected HIF-1α$^{-/-}$ mice showed defective expression of microbicidal effectors and inflammatory cytokines[19]. Contrastingly, Resende *et al.* did not report a difference in bacterial loads between WT and conditional HIF-1α$^{-/-}$ mice. However, survival of HIF-1α$^{-/-}$ mice was still lower compared to WT, but due to an increase in pathological lung inflammation[39]. Thus, these *in vivo* models demonstrate potential for HIF-1α as a target for host-directed therapy, but timing of such treatment seems important for its effectiveness. Baay-Guzman *et al.* have shown that blocking HIF-1α expression during the early stage of TB worsened disease outcome in a progressive pulmonary TB mouse model, while during the late stage it induced apoptosis of infected macrophages and reduced Mtb loads in the lungs of the mice[40]. This suggests that stabilization of HIF-1α could potentially be an effective treatment during the early stage of pulmonary TB.

In summary, additional research is needed to determine if the currently used protocol to measure HIF-1α expression with flow cytometry can be improved. Furthermore, the effects of HIF-1α expression in macrophages, but also in other cell types such as T cells and DCs, need to be further defined to determine whether HIF-1α modulation could be an effective adjunct treatment for (drug-resistant) TB.

References

1. World Health Organization. *Global Tuberculosis Report*. (2022).
2. Pai, M. *et al.* Tuberculosis. *Nat. Rev. Dis. Prim.* **2**, 1–23 (2016).
3. Furin, J., Cox, H. & Pai, M. Tuberculosis. *Lancet* **393**, 1642–1656 (2019).
4. Kolloli, A. & Subbian, S. Host-Directed Therapeutic Strategies for Tuberculosis. *Front. Med.* **4**, 171 (2017).
5. Ayodele, S., Kumar, P., van Eyk, A. & Choonara, Y. E. Advances in Immunomodulatory Strategies for Host-Directed Therapies in Combating Tuberculosis. *Biomed. Pharmacother.* **162**, 114588 (2023).
6. Mosser, D. M. & Edwards, J. P. Exploring the Full Spectrum of Macrophage Activation. *Nat. Rev. Immunol.* **8**, 958–969 (2008).
7. Gordon, S. Alternative Activation of Macrophages. *Nat. Rev. Immunol.* **3**, 23–35 (2003).
8. Mily, A. *et al.* Polarization of M1 and M2 Human Monocyte-Derived Cells and Analysis with Flow Cytometry upon Mycobacterium tuberculosis Infection. *J. Vis. Exp.* **163**, 1–20 (2020).
9. Brighenti, S. & Joosten, S. A. Friends and Foes of Tuberculosis: Modulation of Protective Immunity. *J. Intern. Med.* **284**, 125–144 (2018).
10. Rao Muvva, J., Parasa, V. R., Lerm, M., Svensson, M. & Brighenti, S. Polarization of Human Monocyte-Derived Cells With Vitamin D Promotes Control of Mycobacterium tuberculosis Infection. *Front. Immunol.* **10**, (2020).
11. Palazon, A., Goldrath, A. W., Nizet, V. & Johnson, R. S. HIF Transcription Factors, Inflammation, and Immunity. *Immunity* **41**, 518 (2014).
12. McGettrick, A. F. & O'Neill, L. A. J. The Role of HIF in Immunity and Inflammation. *Cell Metab.* **32**, 524–536 (2020).
13. Taylor, C. T. & Scholz, C. C. The Effect of HIF on Metabolism and Immunity. *Nat. Rev. Nephrol.* **18**, 573–587 (2022).
14. Cramer, T. *et al.* HIF-1α Is Essential for Myeloid Cell-Mediated Inflammation. *Cell* **112**, 645–657 (2003).
15. Terán, G. *et al.* High Glucose and Carbonyl Stress Impair HIF-1-Regulated Responses and the Control of Mycobacterium tuberculosis in Macrophages. *MBio* **13**, (2022).
16. Osada-Oka, M. *et al.* Metabolic adaptation to glycolysis is a basic defense mechanism of macrophages for Mycobacterium tuberculosis infection. *Int. Immunol.* **31**, 781 (2019).
17. Zenk, S. F., Hauck, S., Mayer, D., Grieshober, M. & Stenger, S. Stabilization of Hypoxia-Inducible Factor Promotes Antimicrobial Activity of Human Macrophages Against Mycobacterium tuberculosis. *Front. Immunol.* **12**, 1–11 (2021).
18. Belton, M. *et al.* Hypoxia and Tissue Destruction in Pulmonary TB. *Thorax* **71**, 1145 (2016).
19. Braverman, J., Sogi, K. M., Benjamin, D., Nomura, D. K. & Stanley, S. A. HIF-1α Is an Essential Mediator of IFN-γ–Dependent Immunity to Mycobacterium tuberculosis. *J. Immunol.* **197**, 1287–1297 (2016).

20. Braverman, J. & Stanley, S. A. Nitric Oxide Modulates Macrophage Responses to M. tuberculosis Infection Through Activation of HIF-1α and Repression of NF-kB. *J. Immunol.* **199**, 1805 (2017).

21. Dis, E. Van *et al.* IFN-γ-Independent Control of M. tuberculosis Requires CD4 T Cell-Derived GM-CSF and Activation of HIF-1α. *PLoS Pathog.* **18**, (2022).

22. Li, F. *et al.* Early Secreted Antigenic Target 6-kDa from Mycobacterium tuberculosis Enhanced the Protective Innate Immunity of Macrophages Partially via HIF1α. *Biochem. Biophys. Res. Commun.* **522**, 26–32 (2020).

23. Li, Q. *et al.* Activation of Hypoxia-Inducible Factor 1 (HIF-1) Enhanced Bactericidal Effects of Macrophages to Mycobacterium tuberculosis. *Tuberculosis* **126**, 102044 (2021).

24. Phelan, J. J. *et al.* Desferrioxamine Supports Metabolic Function in Primary Human Macrophages Infected With Mycobacterium tuberculosis. *Front. Immunol.* **11**, 836 (2020).

25. Sohrabi, Y. *et al.* LXR Activation Induces a Proinflammatory Trained Innate Immunity-Phenotype in Human Monocytes. *Front. Immunol.* **11**, (2020).

26. Zheng, H. *et al.* Genetic Basis of Virulence Attenuation Revealed by Comparative Genomic Analysis of Mycobacterium tuberculosis Strain H37Ra versus H37Rv. *PLoS One* **3**, e2375 (2008).

27. Swisher, J. F. A. & Feldman, G. M. The Many Faces of FcγRI: Implications for Therapeutic Antibody Function. *Immunol. Rev.* **268**, 160–174 (2015).

28. Liu, R. *et al.* HIF-1 Stabilization in T Cells Hampers the Control of Mycobacterium tuberculosis Infection. *Nat. Commun.* **13**, (2022).

29. Rodrigues, T. S. *et al.* Mycobacterium tuberculosis-Infected Alveolar Epithelial Cells Modulate Dendritic Cell Function Through the HIF-1α-NOS2 Axis. *J. Leukoc. Biol.* **108**, 1225–1238 (2020).

30. McCaffrey, E. F. *et al.* The Immunoregulatory Landscape of Human Tuberculosis Granulomas. *Nat. Immunol.* **23**, 318 (2022).

31. Ashenafi, S. *et al.* Immunosuppressive Features of the Microenvironment in Lymph Nodes Granulomas from Tuberculosis and HIV-Co-Infected Patients. *Am. J. Pathol.* **192**, 653–670 (2022).

32. Ashenafi, S. & Brighenti, S. Reinventing the Human Tuberculosis (TB) Granuloma: Learning from the Cancer Field. *Front. Immunol.* **13**, (2022).

33. Anand, K. *et al.* Mycobacterial Infections due to PD-1 and PD-L1 Checkpoint Inhibitors. *ESMO Open* **5**, 866 (2020).

34. Aguilo, N. *et al.* Reactogenicity to Major Tuberculosis Antigens Absent in BCG Is Linked to Improved Protection against Mycobacterium tuberculosis. *Nat. Commun.* **8**, (2017).

35. Golovkine, G. R. *et al.* Autophagy Restricts Mycobacterium tuberculosis During Acute Infection in Mice. *Nat. Microbiol. 2023 85* **8**, 819–832 (2023).

36. Genoula, M. *et al.* Fatty Acid Oxidation of Alternatively Activated Macrophages Prevents Foam Cell Formation, but Mycobacterium tuberculosis Counteracts This Process via HIF-1α Activation. *PLoS Pathog.* **16**, (2020).

37. Kotze, L. A. *et al.* Establishment of a Patient-Derived, Magnetic Levitation-Based, Three-Dimensional Spheroid Granuloma Model for Human Tuberculosis. *mSphere* **6**, (2021).

38. Shi, L. *et al.* Infection with Mycobacterium tuberculosis Induces the Warburg Effect in Mouse Lungs. *Sci. Rep.* **5**, 18176 (2015).

39. Resende, M. *et al.* Myeloid HIF-1α Regulates Pulmonary Inflammation During Experimental Mycobacterium tuberculosis Infection. *Immunology* **159**, 121 (2020).

40. Baay-Guzman, G. J. *et al.* Dual role of hypoxia-inducible factor 1 α in experimental pulmonary tuberculosis: Its implication as a new therapeutic target. *Future Microbiol.* **13**, 785–798 (2018).

Supplementary Materials

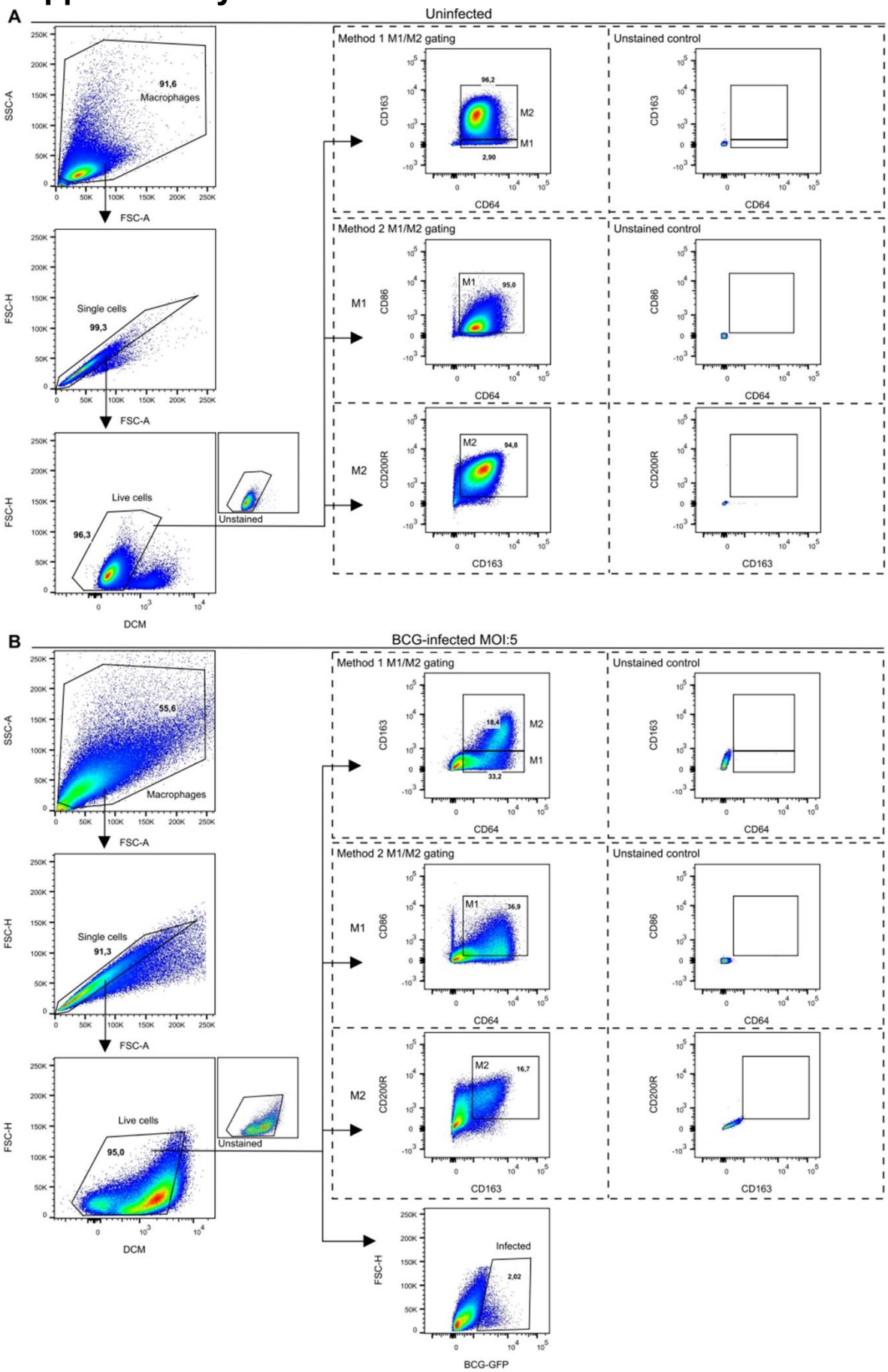

Supplementary figure 1. Gating strategy for flow cytometry. *A) Example of gating strategy for uninfected cells. First, the macrophage population was gated based on SSC and FSC, followed by selection of single cells. To determine the live cell population, the unstained control was used to set the gate in the channel for the dead cell marker (DCM). Live cells were used for determination of MFI of the single markers (not shown). In addition, M1/M2 phenotypes were selected using two methods. Method 1 gated CD64+CD163- M1 cells and CD64+CD163+ M2 cells. Method 2 gated CD86+CD64+ M1 cells and CD200R+CD163+ M2 cells. For both methods, the unstained control was used to set the gate. B) shows an example of the same gating strategy in BCG-infected cells at MOI:5. In addition, infected cells were gated within the live cell population. For infection with BCG at MOI:5 and for H37Ra at MOI:1 and MOI:5 the same gating strategy was used (not shown). Numbers in* ***bold*** *indicate the percentage of a population from its parent population.*